
Increasing the adversarial robustness of capsule networks through scaled distance agreements

David Peer

University of Innsbruck
d.peer@uibk.ac.at

Sebastian Stabinger

University of Innsbruck
sebastian@stabinger.name

Antonio Rodriguez-Sanchez

University of Innsbruck
antonio.rodriguez-sanchez@uibk.ac.at

Abstract

The capsule of a capsule network represents an object or part of an object in a parse tree. An output vector of a capsule encodes the *instantiation parameters* such as position, size, or orientation. The most used algorithm to route vectors from the lower level layers to the upper level layers is the *routing-by-agreement* algorithm. This algorithm is thought to activate capsules in the network such that all active capsules form a parse tree. This parse tree structure should represent a hierarchical composition of objects that are build out of smaller objects. In this paper we introduce different metrics to evaluate the parse tree structure of capsule networks and show that the commonly used routing-by-agreement algorithm does not ensure the emergence of a parse tree. Therefore, we introduce a new routing algorithm named *scaled-distance-agreement routing* that calculates agreements with distances rather than the dot product. We show experimentally for different network architectures and datasets that this new calculation of the agreement ensures a parse tree structure. The novel routing algorithm is also much more robust against whitebox adversarial attacks than the original routing algorithm.

1 Introduction

Convolutional neural networks (CNNs) usually contain pooling layers to reduce their computational complexity while providing translation invariance. As a side effect they lose information about feature locations. To detect objects in upper level layers it is important for neurons to make good use of the precise positions of different lower level parts of the respective object. Preserving the location information of detected features would therefore be desirable, but is hard to achieve in the context of CNNs.

Position is only one of a whole set of parameters describing the features of an object; Size, rotation, and scale being other examples of the so called *instantiation parameters*. An elegant way to deal with these instantiation parameters was introduced by Hinton et al. (2011). The scalar-output neurons are replaced with vector-output *capsules*. A capsule represents an object or part of an object, and the *activity-vector* of the capsule encodes the instantiation parameters of this part. Hinton et al. (2011) hypothesise that, even if the viewing condition of an object changes, the same capsules stay active, representing the same parts with changed instantiation parameters. This property is called *equivariance*.

This viewpoint-equivariance can be used to build relationships between capsules of different layers to solve the problem of assigning parts to wholes. Sabour et al. (2017) introduced an algorithm

Algorithm 1 Routing-by-agreement algorithm as presented by Sabour et al. (2017).

\forall capsules i in layer l and j in layer $l + 1$ with r routing iterations and predictions $\hat{u}_{j|i}$

```

1: procedure ROUTINGBYAGREEMENT( $\hat{u}_{j|i}, r, l$ )
2:    $\forall b_{ij}, b_{ij} \leftarrow 0$ 
3:   for  $r$  iterations do
4:      $c_{ij} \leftarrow \frac{\exp(b_{ij})}{\sum_k \exp(b_{ik})}$ 
5:      $s_j \leftarrow \sum_i c_{ij} \hat{u}_{j|i}$ 
6:      $v_j \leftarrow \frac{\|s_j\|^2}{1 + \|s_j\|^2} \frac{s_j}{\|s_j\|}$ 
7:      $b_{ij} \leftarrow b_{ij} + v_j \cdot \hat{u}_{j|i}$ 
8:   end for
9: end procedure

```

called *routing-by-agreement* (RBA) that creates this relationship iteratively. The output of a capsule should be routed only to the single appropriate parent. An active capsule can therefore be interpreted as a node in a parse tree.

To measure how closely the routing between capsules matches the structure of a parse tree and how dynamic this parse tree is (i.e. to what extent different inputs change the structure of the parse tree), we define two metrics. We will also introduce a new routing algorithm named *scaled-distance-agreement* (SDA) routing that selects a single parent over multiple parent capsules, ensuring that the information in the capsule network is routed according to the structure of a parse tree. Experimentally we also found out that capsule networks where the routing follows a parse tree structure are more robust against white box adversarial attacks in comparison to capsule networks with fully connected routing.

The next chapter will summarize related work. Metrics to evaluate the parse tree structure are presented in section 3. Our novel routing algorithm, ensuring the parse tree structure of capsules, is introduced in section 4. In section 5 we describe and discuss the results of our experiments.

2 Related Work

Capsules, and the idea of equivariant instantiation parameters, were introduced by Hinton et al. (2011), where the authors also showed how such a capsule can be trained by backpropagating the difference between the actual and the target outputs. Later, Sabour et al. (2017) introduced an architecture named CapsNet containing two layers of such capsules. The authors also presented an iterative routing algorithm called routing-by-agreement to route the instantiation parameters between different capsule layers as shown in algorithm 1. The coupling coefficient c_{ij} represents a probability to couple from a lower level capsule i to upper level capsule j and is calculated using the dot product between the predicted vector $\hat{u}_{j|i}$ and the current activation v_j of the capsule. The authors hypothesize that this ensures a lower level capsule coupling with the most appropriate parent capsule of the next layer in such a way that a parse-tree structure is established during routing.

A different routing algorithm was developed by Hinton et al. (2018), which is based on the Expectation-Maximization algorithm. One reason the original routing-by-agreement algorithm is still popular and often used in later work is likely it’s ease of implementation in common deep learning frameworks. In addition, the algorithm is easily adapted to meet new requirements. Some applications that use the routing-by-agreement algorithm include the works of Mobiny and Nguyen (2018) for lung cancer screening, Duarte et al. (2018) for detecting actions in videos or Rawlinson et al. (2018) for unsupervised learning. This latter work provided an interesting insight into the routing-by-agreement algorithm, namely that a missing mask causes the loss of equivariance as well as other desired qualities of capsule networks. The authors started with the assumption that routing-by-agreement produces a parse-tree and therefore only used the largest coupling coefficient by masking out all capsules other than the parent. The validity of this assumption will be evaluated in this paper.

Ancheng et al. (2018) evaluated the accuracy of a capsule network using a different number of routing iterations and found that the entropy of the coupling coefficient decreases as the training progresses. The authors also found that routing is mostly random at the beginning of training, and

suggest that a capsule should not be too confident about its parent capsule in the early training stage, or it might lead to bad performance of the network. They called this issue *early over routing*. In their experiments they also measured the entropy of the coupling coefficients. The authors showed that the entropy is still large after 7 routing iterations, indicating that a capsule sends its activity vector to multiple capsules in the following layer and not only to one parent capsule. A normalized metric, measuring the same property, that is independent of the number of capsules is introduced in the next section.

3 Metrics for dynamic parse-tree evaluation

A dynamic routing algorithm for capsule networks should have the following properties:

1. *Parse tree structure*: During inference, the routing algorithm should activate capsules in the network such that each one represents a node in a parse tree. Therefore, a capsule should only be coupled to one parent for a single input example, but one parent can be coupled to multiple children.
2. *Dynamicity*: The routing algorithm should select the parent capsule based on the current input. The coupling of lower level capsules with parent capsules should be dynamic and the parse tree should change for different inputs.

In the following paragraphs we describe metrics to measure desired properties of a capsule network routing algorithm:

Measuring parse tree quality To show the existence of a parse tree structure and measure its quality, the coupling coefficient c_{ij} have to be analyzed. For all lower level capsules there should exist only one preferred capsule, the parent node, in the parse tree. The coupling to all other capsules in the layer above should be small.

Therefore, a parse tree is created whenever the entropy of c_{ij} from a lower level capsule i to an upper level layer is small. The calculation of the average entropy for a mini-batch of training examples is shown in equation (1) for a single layer.

For I capsules in layer l and J capsules in layer $l + 1$, the average entropy for a mini-batch with M training examples for a single layer can be calculated with

$$H_{\text{avg}} = \frac{1}{MI} \sum_{m=1}^M \sum_{i=1}^I \sum_{j=1}^J -c_{ij}^m \log c_{ij}^m \quad (1)$$

where c_{ij}^m is the coupling in example m from the lower level capsule i to the upper level capsule j .

Changing the number of capsules also changes the measured entropy. This can be prevented by normalizing the entropy using the maximum possible entropy $\log J$ where J is the number of capsules in layer l . The normalized metric is shown in equation (2) and is close to 1 whenever a parse tree is created and close to 0 whenever capsules are uniformly coupled.

$$T = 1 - \frac{H_{\text{avg}}}{\log J} \quad (2)$$

Measuring dynamicity Dynamicity measures how much the parse tree structure changes with respect to changes in the input. It can be measured using the difference of the minimum and maximum value between coupling coefficients of different input examples. The calculation of this metric is shown in equation (3). For I capsules in layer L , J capsules in layer $L + 1$ and M training examples:

$$D = \frac{1}{IJ} \sum_{i=1}^I \sum_{j=1}^J \left(1 - \frac{\min_{m=1}^M (c_{ij}^m)}{\max_{m=1}^M (c_{ij}^m)} \right) \quad (3)$$

where $\min_{m=1}^M$ is the minimum value between 1 and M examples of a mini-batch with size M and $\max_{m=1}^M$ being the maximum value. Dynamicity is close to 1 whenever the structure of the routed capsules changes with different input examples and close to 0 when the structure is static. This

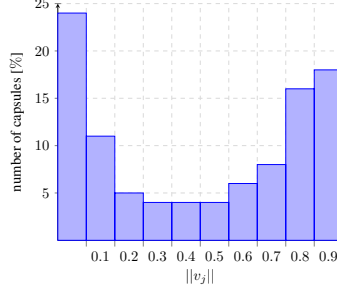


Figure 1: Histogram of $\|v_j\|$ for the second hidden layer of a capsule network with multiple layers as described in section 5. This histogram shows that the number of inactive capsules is large for a network trained on the classical MNIST dataset.

metric is independent of the exact structure of the routed capsules such that the dynamicity can still be large even when the routed capsules do not form a parse tree.

4 Scaled-distance-agreement routing

We will now present a novel routing algorithm that satisfies the aforementioned properties of a good routing algorithm. We call it the *scaled-distance-agreement* (SDA) routing algorithm.

The RBA algorithm calculates the log prior probability with $b_{ij} = b_{ij} + \cos(\alpha) \|v_j\| \|\hat{u}_{j|i}\|$ where α is the angle between both vectors. The activity vector v_j is the nonlinear sum of all lower level predictions weighted by the coupling coefficient c_{ij} . The prediction $\hat{u}_{j|i} = W_{ij}u_i$ is created from lower a level capsule i to an upper level capsule j using the transformation matrix W_{ij} .

A disadvantage of this method is that whenever the prediction vector $\hat{u}_{j|i}$ is large, the calculated b_{ij} also becomes large and the angle between both vectors has less influence on the coupling. This means that b_{ij} can be increased by simply increasing the values in the weight matrix W_{ij} without actually decreasing the angle, and therefore increasing the agreement, between the parent and child capsule.

We can avoid this problem by normalizing $v_j \cdot \hat{u}_{j|i}$ by $\|v_j\|$. Unfortunately we could experimentally show that this normalization does not ensure a parse tree structure. We hypothesize that this normalization does not achieve it's goal due to a second disadvantage: In a parse tree structure a capsule should be active if the corresponding object is present, otherwise the capsule should be inactive. Therefore, during inference with a single input example, many active as well as many inactive capsules exist in a single layer. We tested this for the MNIST dataset by plotting a histogram of $\|v_j\|$ as shown in figure 1. All those inactive capsules have random directions because the respective object does not exist and predictions are guessed. Therefore with a high probability for some predictions of an active lower level capsule, there exists an inactive upper level capsule with a similar direction which produces a large agreement between both capsules. In the next routing iteration this coupling activates the inactive capsule such that multiple parents exists which violates the parse tree structure.

To avoid this problem we use distances instead of the dot product such that an inactive and an active capsule disagree and therefore produce a coupling coefficient c_{ij} which is smaller than $\frac{1}{J}$. Distances also ensure that a large transformation matrix W_{ij} does not automatically produce a large agreement. To utilize this insight, algorithm 1 must be modified as follows: The length of the activity vector v_j represents the probability of an entity being present. Therefore, we keep the non-linearity from Sabour et al. (2017) as shown in line 7 of algorithm 1. This nonlinearity ensures that the length of the vector represents a probability and that it satisfies $0 \leq \|v_j\| \leq 1$. This leads to all activity vectors being contained within an n-dimensional hypersphere of radius 1, where the maximum possible distance between the prediction and the output vector is 2. The maximum distance is reached when $\hat{u}_{j|i} = -v_j$. So, the maximum possible coupling coefficient for the parent capsule will be reached whenever $\|\hat{u}_{j|i} - v_j\| = 0$ for the parent capsule and $\|\hat{u}_{j|i} - v_j\| = 2$ for all other capsules. The maximum coupling coefficient that is possible for the parent capsule with e.g. 10 upper level capsules is therefore 0.45. This maximum coupling coefficient gets worse as the number of upper

Algorithm 2 Scaled-distance-agreement routing algorithm.

\forall capsules i in layer l with I capsules and j in layer $l + 1$ with J capsules, r routing iterations and predictions $\hat{u}_{j|i}$

```

1: procedure SDAROUTING( $\hat{u}_{j|i}$ ,  $r$ ,  $l$ )
2:    $\forall b_{ij}, b_{ij} \leftarrow 0$ 
3:   for  $r$  iterations do
4:      $c_{ij} \leftarrow \frac{\exp(b_{ij})}{\sum_k \exp(b_{ik})}$ 
5:      $c_{ij} \leftarrow \begin{cases} c_{ij} & \text{if } c_{ij} \geq \frac{1}{J} \\ 0 & \text{otherwise} \end{cases}$ 
6:      $s_j \leftarrow \frac{1}{J} \sum_i c_{ij} \hat{u}_{j|i}$ 
7:      $v_j \leftarrow \frac{\|s_j\|^2 s_j}{1 + \|s_j\|^2 \|s_j\|}$ 
8:      $t_i \leftarrow \frac{\log(0.9(J-1)) - \log(1-0.9)}{-0.5 \text{mean}_j(\|\hat{u}_{j|i} - v_j\|)}$ 
9:      $b_{ij} \leftarrow \|\hat{u}_{j|i} - v_j\| t_i$ 
10:  end for
11: end procedure

```

level layer capsules increases. For 128 capsules, the maximum possible value for c_{ij} for the parent capsule decreases to 0.05.

To be able to represent a parse tree structure, we first multiply the distance by a scale factor t to allow larger coupling coefficients for the parent capsule. This factor is set to a value so that the parent capsule couples with probability c_{ip} whenever the euclidean distance of the parent prediction is d_p and the distance to all other capsules is d_o where $d_p < d_o$. The coupling coefficient is calculated using the *softmax* function. Therefore, c_{ip} satisfies

$$c_{ip} = \frac{\exp(b_{ij})}{\sum_k \exp(b_{ik})} = \frac{\exp(d_p t)}{\sum_{J-1} \exp(d_o t) + \exp(d_p t)} \quad (4)$$

where J is the number of parent capsules. By rewriting equation (4) we can calculate the scale factor t with

$$t = \frac{\log(c_{ip}(J-1)) - \log(1 - c_{ip})}{d_p - d_o} \quad (5)$$

Note that the scaling factor t is negative so that small distances produce a large agreement and large distances a small agreement. Empirically we found that setting $c_{ip} = 0.9$ whenever $d_p = \frac{d_o}{2}$ where $d_o \approx \text{mean}(\|\hat{u}_{j|i} - v_j\|)$ produces a strong coupling to the parent capsule, but still allows a uniform coupling at the beginning of training. This is important to avoid early over routing. The calculation of the agreement using this scaled distance is shown in line 8 and line 9 of algorithm 2.

Using those scaled distances as an agreement measure we can now separate predictions between inactive capsules and active capsules. This separation is shown in line 5 of algorithm 2. More precisely, all prediction vectors $\hat{u}_{j|i}$ which have a coupling $c_{ij} \geq \frac{1}{J}$ are used for the calculation of upper level instantiation vectors. So, in the first iteration, the activity vector for one upper level capsule j is the average of all predictions because $c_{ij} = \frac{1}{J}$. After the first iteration, the coupling from lower level capsules to upper level capsules with large distances will be decreased and increased for capsules with smaller distances. Therefore, c_{ij} increases when active predictions agree with other active lower level capsule predictions and c_{ij} decreases if it disagrees with other predictions i.e. if those are inactive. Additionally in the next iteration, the activation vector is calculated only with predictions that agree with each other and therefore v_j is calculated without the negative influence of wrong predictions.

Another important change compared to the algorithm from Sabour et al. (2017) is that we scale s_j by $\frac{1}{J}$ before we apply the nonlinearity as shown in line 6 of algorithm 2. The reason for this scaling is that the values of c_{ij} are close to uniform in the original algorithm. For the novel routing algorithm this coefficient is much larger so that after the nonlinearity, the activation is pushed towards the

Table 1: Comparison of metrics defined in section 3 for the CapsNet architecture evaluated on the MNIST test set averaged for all layers.

| Routing | T | D | Accuracy |
|---------|--------------|-------------|--------------|
| Uniform | 0.000 | 0.00 | 99.64 |
| RBA | 0.001 | 0.11 | 99.76 |
| SDA | 0.843 | 0.99 | 99.62 |

saturated region of the nonlinearity. We avoid this by scaling the length of the vector by the same factor as in the original case which is $\frac{1}{J}$ for J output capsules.

The combination of the distance to calculate the agreement and the separation of active and inactive instantiation vectors ensures that the distance from calculated activation vectors to parent predictions decrease as the routing proceeds. Therefore the coupling to parent capsules increases and a parse tree structure is formed during the routing process. In the next section we show that the activity vector also changes between different training examples and so the routing algorithm is dynamic too.

5 Experimental evaluation

Using the metrics introduced in section 3, we evaluate the structure of active capsules, the performance and the adversarial robustness in this section. We compare the routing-by-agreement algorithm, the scaled distance agreement routing and a routing where all capsules are uniformly coupled ($c_{ij} = \frac{1}{J}$ for J output capsules). We used the MNIST dataset from LeCun and Cortes (2010), fashionMNIST from Xiao et al. (2017) and smallNorb from LeCun et al. (2004) in all experiments.

5.1 Architecture

Two different architectures are used to run the experiments. The first consists of only two capsule layers: A primary layer and the output layer. This is the same architecture presented by Sabour et al. (2017). We refer to this architecture as *CapsNet*.

The second architecture uses two additional hidden capsule layers between the primary and output caps layer. The first hidden capsule layer consists of 24 capsules with dimension 10 and the second of 20 capsules with dimension 12. The output layer has dimension 16 with 10 capsules for MNIST and FashionMNIST and 5 capsules for the smallNorb dataset. We refer to this architecture as the *two hidden layer model*.

5.2 Setup

We used the original implementation of CapsNet provided by Sabour et al. (2017) (available from GitHub¹) for all experiments. Our implementation, a link to the datasets that we used, and a link to the the trained networks are available on GitHub².

All experiments used TensorFlow 1.12.0 from Abadi et al. (2015) and ran on a single *Nvidia-Titan XP* GPU. The following hyperparameters were used: Batch size of 128, the Adam optimizer with a decay rate of 0.96, a learning rate of 0.001 and 3 routing iterations.

5.3 Evaluating the parse tree structure

The authors of the routing-by-agreement algorithm provide the weights of CapsNet trained on MNIST. In this experiment we compare this original model with SDA routing and with uniform routing. The model that uses SDA routing and uniform coupling between capsules is evaluated on MNIST after 120k training steps. As shown in table 1 the parse tree structure of the tested network

¹Sabour S. (2018, September 11). *Original GitHub Repository of CapsNet TensorFlow implementation*. From <https://github.com/Sarasra/models/tree/984fbc754943c849c55a57923f4223099a1ff88c>

²Original link removed for review. Source code, links to the dataset and links to download the trained networks are added to the supplementary material (see file README.md)

Table 2: Comparison of routing-by-agreement, scaled-distance-agreement routing and uniform routing for the two hidden capsule layer architecture averaged for all layers on the respective test set.

| Dataset | Routing | T | D | Accuracy |
|--------------|---------|-------------|-------------|--------------|
| MNIST | Uniform | 0.00 | 0.00 | 99.59 |
| | RBA | 0.06 | 0.76 | 99.62 |
| | SDA | 0.57 | 0.93 | 99.38 |
| FashionMNIST | Uniform | 0.00 | 0.00 | 92.11 |
| | RBA | 0.05 | 0.80 | 91.46 |
| | SDA | 0.55 | 0.97 | 90.85 |
| smallNORB | Uniform | 0.00 | 0.00 | 93.59 |
| | RBA | 0.05 | 0.70 | 92.23 |
| | SDA | 0.62 | 0.99 | 89.23 |

with routing-by-agreement is much closer to a uniform routing than to the actually desired routing to a single parent. Also the dynamicity is very low, which shows that a capsule couples always with the same parent capsules or with all capsules in the case of uniform coupling independent of the input.

The SDA based routing has a parse tree metric close to 1 indicating that the structure of all active capsules form a parse tree. The dynamicity metric of 0.99 shows that the parse tree structure also changes with different input examples. We can also see that the accuracy of the SDA routing, RBA and uniform coupling are very close.

5.4 Evaluating two hidden layers

In the first experiment we evaluated the routing algorithms on the CapsNet architecture. In this experiment we evaluate the structure of capsules on the two hidden layer network. Additionally, we check if a parse tree structure also emerges for FashionMNIST and the smallNORB dataset. We trained the network on FashionMNIST for 120k steps and on smallNORB for 160k steps. From the results in table 2 we can observe the following: The uniform routing has no parse tree structure and is not dynamic but has the best performance on FashionMNIST and smallNORB but RBA outperforms uniform coupling by 0.12% on MNIST. In all experiments the RBA algorithm produces close to uniform coupling, but the coupling still changes between input examples. This indicates that no parse tree structure is created, although the routing algorithm is dynamic. In all experiments, the SDA routing creates the strongest parse tree structure and is also more dynamic than RBA which shows that the algorithm works as designed. Another interesting observation is, that the accuracy decreases slightly as capsules form a parse tree structure.

5.5 Evaluating adversarial robustness

In a third experiment we compared the robustness against whitebox adversarial attacks of all routing algorithms and datasets for the two hidden layer network. We compared the accuracy after applying the *fast sign gradient method* (FGSM) from Goodfellow et al. (2015) to the test set. This method changes the pixel intensity by ϵ into the direction of the sign of the gradient such that the loss is increased. Therefore we compared to robustness for different values of ϵ . The results for $\epsilon = \{0.1, 0.2, 0.3, 0.4, 0.5\}$ are shown in table 3 where we can conclude that: For all values of ϵ SDA routing outperformed RBA and uniform coupling. SDA routing outperformed uniform routing on average by 24.48% for MNIST, 24.29% for FashionMNIST and 4.83% for smallNorb. SDA routing outperformed routing-by-agreement on average by 18.48% for MNIST, 14.12% for FashionMNIST and 5.06% for smallNorb. In almost all cases a stronger parse tree structure also implies that the adversarial robustness increases. Only for the smallNorb dataset with $\epsilon = 0.1, 0.2$ uniform coupling outperformed RBA.

Table 3: Accuracy for different ϵ values after an FSGM attack is applied on the MNIST, Fashion-MNIST and smallNorb test set. Compared on the two hidden layer architecture for the routing-by-agreement, scaled-distance-agreement routing and uniform routing algorithm.

| Dataset | Routing | FSGM Attack (ϵ) | | | | |
|--------------|---------|----------------------------|--------------|--------------|--------------|--------------|
| | | 0.1 | 0.2 | 0.3 | 0.4 | 0.5 |
| MNIST | Uniform | 77.53 | 34.64 | 17.54 | 11.61 | 09.08 |
| | RBA | 82.73 | 46.48 | 23.93 | 15.61 | 11.68 |
| | SDA | 90.41 | 66.35 | 53.59 | 34.91 | 27.57 |
| FashionMNIST | Uniform | 34.51 | 16.36 | 11.87 | 10.67 | 10.23 |
| | RBA | 36.82 | 25.59 | 32.68 | 20.18 | 19.22 |
| | SDA | 65.22 | 51.74 | 38.32 | 28.46 | 21.40 |
| smallNORB | Uniform | 27.72 | 22.75 | 18.39 | 17.07 | 16.12 |
| | RBA | 26.25 | 21.05 | 18.80 | 17.63 | 17.14 |
| | SDA | 28.16 | 27.44 | 25.65 | 23.43 | 21.58 |

6 Conclusions

In this paper we have shown that the coupling coefficients calculated by the routing-by-agreement algorithm are close to a uniform coupling. We concluded that capsules of such a network do not necessarily represent a parse tree structure.

The different properties that a routing algorithm should have to form a dynamic parse tree structure are also mentioned in this paper. We defined metrics that can be used to measure these properties and created a novel routing algorithm that improves these metrics compared to the routing-by-agreement algorithm.

We showed experimentally that the scaled-distance-agreement routing algorithm in comparison to the routing-by-agreement algorithm creates a dynamic parse-tree structure. We evaluated this for two different architectures and for three different datasets. In those experiments we have also seen that the accuracy is in almost all cases the largest for uniform coupling and decreases slightly as the parse tree structure emerges. Conversely, the accuracy under FSGM adversarial attacks increases as the parse tree structure is created. For example, on MNIST with $\epsilon = 0.3$ the accuracy of SDA is 29.66% larger compared to RBA and 36.05% larger compared to uniform coupling.

References

- Abadi, M., Agarwal, A., Barham, P., Brevdo, E., Chen, Z., Citro, C., Corrado, G. S., Davis, A., Dean, J., Devin, M., Ghemawat, S., Goodfellow, I., Harp, A., Irving, G., Isard, M., Jia, Y., Jozefowicz, R., Kaiser, L., Kudlur, M., Levenberg, J., Mané, D., Monga, R., Moore, S., Murray, D., Olah, C., Schuster, M., Shlens, J., Steiner, B., Sutskever, I., Talwar, K., Tucker, P., Vanhoucke, V., Vasudevan, V., Viégas, F., Vinyals, O., Warden, P., Wattenberg, M., Wicke, M., Yu, Y., and Zheng, X. (2015). TensorFlow: Large-scale machine learning on heterogeneous systems. Software available from tensorflow.org.
- Ancheng, L., Jun, L., and Zhenyuan, M. (2018). On learning and learned representation with dynamic routing in capsule networks. abs/1805.04041.
- Duarte, K., Rawat, Y. S., and Shah, M. (2018). Videocapsulenet: A simplified network for action detection. abs/1805.08162.
- Goodfellow, I. J., Shlens, J., and Szegedy, C. (2015). Explaining and harnessing adversarial examples.
- Hinton, G. E., Krizhevsky, A., and Wang, S. D. (2011). Transforming auto-encoders. In *ICANN*.
- Hinton, G. E., Sabour, S., and Frosst, N. (2018). Matrix capsules with em routing. In *ICLR*.
- LeCun, Y. and Cortes, C. (2010). MNIST handwritten digit database.
- LeCun, Y., Huang, F. J., and Bottou, L. (2004). Learning methods for generic object recognition with invariance to pose and lighting. In *CVPR (2)*, pages 97–104.

- Mobiny, A. and Nguyen, H. V. (2018). Fast capsnet for lung cancer screening. In Frangi, A. F., Schnabel, J. A., Davatzikos, C., Alberola-López, C., and Fichtinger, G., editors, *MICCAI (2)*, volume 11071 of *Lecture Notes in Computer Science*, pages 741–749. Springer.
- Rawlinson, D., Ahmed, A., and Kowadlo, G. (2018). Sparse unsupervised capsules generalize better. [abs/1804.06094](#).
- Sabour, S., Frosst, N., and Hinton, G. E. (2017). Dynamic routing between capsules. In Guyon, I., von Luxburg, U., Bengio, S., Wallach, H. M., Fergus, R., Vishwanathan, S. V. N., and Garnett, R., editors, *NIPS*, pages 3859–3869.
- Xiao, H., Rasul, K., and Vollgraf, R. (2017). Fashion-mnist: a novel image dataset for benchmarking machine learning algorithms.